Proceedings of 5th Jagiellonian Symposium on Advances in Particle Physics and Medicine, Kraków, Poland, 2024

Indication of High-Energy Leptons (e^+/e^-) Originating from the DD Fusion Reaction at Very Low Energy

R. Dubey[a,*], K. Czerski[a], H. Gokul Das[a], A. Kowalska[b], N. Targosz-Sleczka[a], M. Kaczmarski[a] and M. Valat[a]

[a]*Institute of Physics, University of Szczecin, 70-451 Szczecin, Poland*
[b]*Institute of Mathematics, Physics and Chemistry, Maritime University of Szczecin, 70-500 Szczecin, Poland*

Doi: 10.12693/APhysPolA.146.716 *e-mail: rakesh.dubey@usz.edu.pl

Following the preliminary indications of electron/positron (e^+/e^-) pair production reported in the deuteron–deuteron reaction, which supported the existence of a single-particle threshold resonance in ^{4}He, a series of experiments have been conducted over the past two years at the eLBRUS Ultra High Vacuum Accelerator Facility at the University of Szczecin, Poland. During certain stages of these experiments, a simple detection system, including silicon (Si) detectors of varying thicknesses and different aluminum (Al) absorption foils placed in front of the detectors, was employed. In addition to Si charged particle detectors, a high-purity germanium detector was used to investigate the effect of internal pair e^+/e^- creation originating from deuteron–deuteron reactions and to determine the branching ratio between emitted protons, neutrons, and e^+/e^- pairs at 12 keV deuteron energies. The measured electron energy spectrum and the electron–proton branching ratio agree with Geant4 Monte Carlo simulations and our theoretical expectations for an electron–positron pair creation decay from the deuteron–deuteron 0^+ threshold resonance to the ground state. Furthermore, according to theoretical predictions, an increase in the electron–proton branching ratio with decreasing deuteron energies could make the electron channel the most dominant at thermal energies, potentially leading to a future fusion energy source based on high-energy electrons.

topics: fusion, electron, positron, annihilation line, internal pair creations

1. Introduction

The fusion of deuterium nuclei within a metallic environment at low energies offers a perspective on the fundamental physical processes governing in stellar plasmas such as those found in giant planets, brown dwarfs, and white dwarfs [1–3]. In this low-energy deuteron–deuteron (DD) fusion regime, the branching ratios of the DD reaction may be significantly influenced by the threshold resonance, a phenomenon primarily attributed to the nucleus's internal structure and characterized by its partial resonance widths [4, 5]. The total resonance width, which is the sum of deuteron, proton, neutron, and electromagnetic partial widths, is strongly energy-dependent due to the penetration factor in the deuteron channel. Theoretical calculations, assuming $J^\pi = 0^+$) and based on the E_0 energy-weighted sum rule, predict a significant partial width for e^+e^- internal pair creation (IPC) at the DD threshold resonance [6]. The contribution of the e^+e^- channel to the DD reaction cross-section is observable at energies of the order of few keV, where electron screening enhances DD reactions by lowering the Coulomb barrier [5, 7].

Recently, another feature of ^{4}He nuclei associated with the proton decay threshold was highlighted [8, 9]. Firstly, experimental studies of the monopole transition of ^{4}He were performed via the ^{4}He level structure at excitation energies below 30 MeV using inelastic electron scattering [8]. Later, N. Michel et al. [9] presented a theoretical argument in the form of a coupled-channel depiction of the no-core Gamow shell model and described the excitation energy and the monopole form factor of the 0^+ state by considering the (^{3}H$+p$), (^{3}He$+n$), and (^{2}H $+^2$ H) reaction channels.

Here, we present part of an experimental measurement compaign on electron emission in low-energy DD reactions, which may originate from the internal pair creation decay of the DD threshold resonance. In this study, a simple detection system with thick-thin Si-charged particle detectors, along with a simultaneous high purity germanium (HPGe) detector setup, is used. The experimental

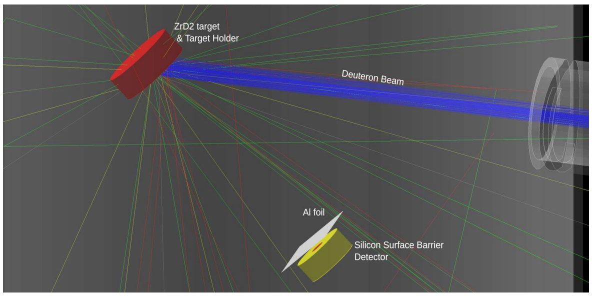

Fig. 1. Detection geometry simulated with GEANT4 and visualized with OpenGL, consisting of a silicon detector, a target, and a target holder [11].

results will be compared with theoretical calculations of the reaction branching ratio, suggesting an e^+e^- transition to the ground state of ^{4}He. Furthermore, the experimental analysis will be supported by Monte Carlo simulations using the Geant4 MC code [10]. A detailed understanding of the various components of the experimental setup has been previously discussed in our work [11].

2. Experimental setup and results

A series of experiments were performed at the eLBRUS Ultra High Vacuum Accelerator Facility at Szczecin University [12], Poland, to re-measure the previously reported indication of electron emission from the DD reaction at very low energy [5]. During these experiments, a deuterium beam was accelerated to energies of 12 keV with a constant beam current of 50 μA using magnetically analyzed single-charged atomic deuterium ions. Zirconium foils (1 mm thick; 99.2% purity) were purchased from Goodfellow GmbH, Hamburg, Germany. The target was prepared by cutting the foils to dimensions of 1.5×2 cm^2 (1 mm thick). In the present studies, the electron-screening effect plays a very important role in the DD fusion process in a metallic environment, and it depends on the formation of a high number of vacancies during the deuteron irradiation of the samples, with minor dependence on carbon and oxygen impurities, which affect the depth distribution of vacancies and their diffusion. Thus, extensive material diagnostics are required to gain better insight into the mechanism. For the present ZrD_2 samples used as targets, we have conducted X-ray diffraction (XRD) and proton-induced X-ray emission (PIXE) characterizations before and after irradiation [13].

The beam was directed onto a 1 mm-thick ZrD_2 target tilted at 45° to the beam, resulting in a beam spot size of 7×12 mm^2. To minimize natural background noise and systematic uncertainties, the experiment started with a simple configuration featuring a single silicon detector, first with a thickness of 100 μm and later 2 mm. Geant4 Monte Carlo simulations were used to discern the distinct effects of direct fusion events from non-fusion events originating from particles elastically scattered within the target and protective foils, such as protons and electrons (e^-) [11].

TABLE I

HPGe detector specifications and performance data; FWHM — full width at half maximum.

Details	Description
detector model	GEM35P4-950
relative efficiency [%]	35
energy resolution (at FWHM) [keV]	1.85
detector material	p-type Ge
crystal diameter [mm]	57.6
crystal length [mm]	65.8
window material and thickness [mm]	Al

The 22.84 MeV IPC originating from the deuterium–deuterium (DD) threshold resonance will produce bremsstrahlung and excess in annihilation peak radiation when it passes through scintillating detecting medium [14]. For this purpose, a large-volume cylindrical HPGe detector with a 58 mm crystal diameter and 66 mm length, providing 35% relative efficiency, was positioned 47 cm from the ZrD_2 target at an angle of 48° with respect to the beam direction. Details of the HPGe setup during the experiments are mentioned in the "Methods section" of the article [7]. Details about the HPGe detector are presented in Table I. HPGe detectors are highly sensitive to the surrounding gamma and light particle environments, which can influence the measured experimental data. We attempted to understand these effects quantitatively at every stage of the accelerator's operation during the measurements. The procedure was as follows: (i) to separate the events between the experimental spectra from accelerator-induced reactions and fusion events produced by the D_2 beam on the ZrD_2 target; and (ii) to separate the background either from the accelerator or the D_2 beam on the ZrD_2 target [14]. Data acquisition was carried out using a single-parameter multi-channel analyzer (MCA), and data were collected on an event-by-event basis for thorough analysis.

2.1. HPGe gamma-ray detector systems

Tennelec model 950 HPGe detector attached to a 30 l liquid nitrogen dewar (ORTEC, Oak Ridge, Tennessee) was used to measure the fusion products from the reactions. Details about specifications and performance data of the HPGe detector are listed in Table I.

All measurements for the energy and efficiency calibration of the gamma spectrometer system were conducted using different standard gamma sources: ^{137}Cs, ^{60}Co, and ^{22}Na, with point source geometry. A bin-based network installation management (NIM) electronic system, along with a multi-channel analyzer (MCA), was used for spectra acquisition and analysis. Statistical errors were considered when calculating the uncertainties in the measurements. The photopeak efficiency of the HPGe detector was determined from the measured spectra by dividing the number of counts per second under the relevant peak area for each detector-source distance by the known radionuclide activity and gamma decay rate.

In addition to the aforementioned experimental setup, the d$E-E$ telescope was used in a certain phase of the measurements. This telescope featured a 300-μm thick silicon (Si) detector for detecting energy loss (dE) and a 5-cm high-purity germanium (HPGe) detector for measuring energy (E) in the high-energy electron range, extending to 8 MeV [15]. However, due to specific limitations in our experimental design, we were unable to place this telescope as close to the target as possible. Consequently, this setup imposed an upper limit on the measured high-energy electrons originating from the DD reaction at very low energy [15].

2.2. Charge particle spectra

In Fig. 2a–b, a comparison between the charged particle energy spectra measured with the thicker 2000 μm and thinner 100 μm Si detectors, having in front 36 μm and 0.4 μm Al absorber foils, respectively, at the same 12 keV deuteron energies is presented. As shown in Fig. 2a, a noticeable bump around 0.7 MeV can be clearly observed, which is nearly ten times weaker than the proton peak. The ^{3}He and triton peaks are missing, because they are fully stopped by the thick 36 μm foil absorber. Protons emitted with an energy of about 3 MeV are shifted to around 1.8 MeV after losing ≈ 1.2 MeV of energy in the foil. The corresponding Geant4 Monte Carlo simulation for the electron–positron emission from the DD threshold resonance during IPC, and its comparison with the experimental spectrum, is presented as a solid red line. The calculations also consider the contribution from scattered protons, which is on the order of 10^{-4} compared to the full energy line of protons [11]. A slight difference in the calculated energy peak position of electrons (nearly 50 keV) can be observed [11]. In the case of the 100 μm thick Si detector spectrum (as shown in Fig. 2b), we observed three known peaks from the DD reaction: the neutron channel (^{3}H$, n$) and the proton channel (^{3}He$, p$). Due to energy loss in the Al absorber foil, ^{3}He has its energy reduced by 231 keV from its original energy of 0.82 MeV, the tritons have their energy reduced by 850 keV from their original energy of 1.02 MeV, and the protons retain nearly their original energy of around 3 MeV.

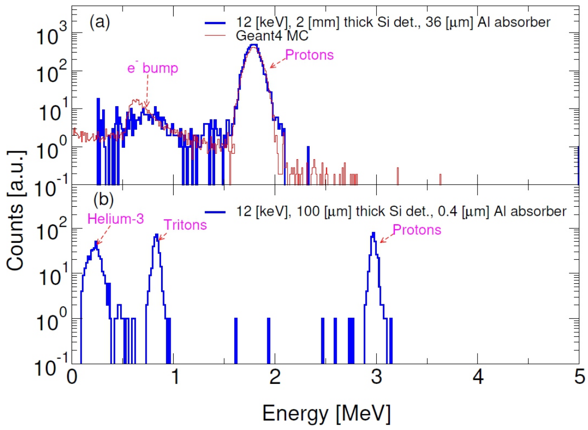

Fig. 2. Experimental energy spectrum measured at deuteron energy 12 keV using (a) 2 mm thick Si detector and 46 μm thick Al absorption foil, (b) 100 μm thick Si detector and 0.4 μm thick Al absorption foil.

2.3. HPGe gamma-ray detector spectrum

In Fig. 3a–b, the experimental energy spectra measured at a deuteron energy of 12 keV using a HPGe detector are presented. In Fig. 3a, we present the full energy spectra measured with the beam, where all the natural background peaks can be seen very clearly. In the obtained photon spectra, it is quite challenging to unfold the spectra to identify the signature of internal pair creation (IPC) from the DD threshold resonance. This difficulty arises because prerequisite steps are needed to separate the neutron-induced gamma spectra and other neutron-related reactions, such as neutron activation, the background spectra including natural gamma contributions and the photons contributions from the accelerator. Another limitation is the size of the HPGe crystal, which must be large enough to absorb the bremsstrahlung from 24 MeV e^-/e^+, and can only absorb a maximum of 11 MeV, as indicated by the Geant4 MC predictions [14]. Below 10 MeV, there is significant overlap of counts from both the background and neutron-induced spectra for such kind of reactions [14, 16].

Therefore, we adopted a simpler approach by focusing on any excess or change in the 511 keV annihilation line during the measurement with respect to the background. Interestingly, there was an excess of counts found to be three orders of magnitude stronger than the accelerator-induced background, as shown in Fig. 3b. Such a strong excess in the 511 keV line might be IPC originating from

TABLE II

The branching ratio (BR) of electron/proton and annihilation peak (AP)/proton was determined for the deuteron energies at 12 keV and compared with theoretical calculations [5, 6].

Deuteron energy [keV]	BR (exper.)			BR (theory [5, 6])
	IPC/proton (100 μm Si det.)	electron/proton (2 mm Si det.)	AP/proton (HPGe)	
12	–	0.15 ± 0.01	0.27 ± 0.08	0.17

the DD threshold resonance; however, better measurements will be performed in coincidence or veto with a charged particle dE–E telescope to observe this effect more carefully. Since the excess of counts in the annihilation line after the accelerator-induced background subtraction is very close to 3.5 sigma, this inhibits us from clearly stating the IPC observations in the DD fusion reactions. The excess of annihilation counts might be due to the external pair creation originating from the neutron flux, which activates gamma rays from various components of the experimental setup, such as the stainless steel chamber or even the Ge crystal. To address this, we first attempted to estimate the total neutron flux emitted during the measurement using charged particle detection with the Si detector. After applying solid angle and efficiency corrections, we found that the neutron flux strength was close to the upper limit of the background. As a result, the change in the annihilation peak due to neutron activation is very close to the background levels. This was further verified with the help of Geant4 Monte Carlo simulations [14, 16]. The interplay between neutron-activated gamma rays and internal pair creation (IPC) from DD fusion in the annihilation peak will be slightly more visible if we use large volumes of NaI detectors for such low-energy measurements [14]. This experiment is currently under preparation in our labolatory. This is our preliminary work, and it can help us determine the initial strength of the signal prior to the coincidence measurement.

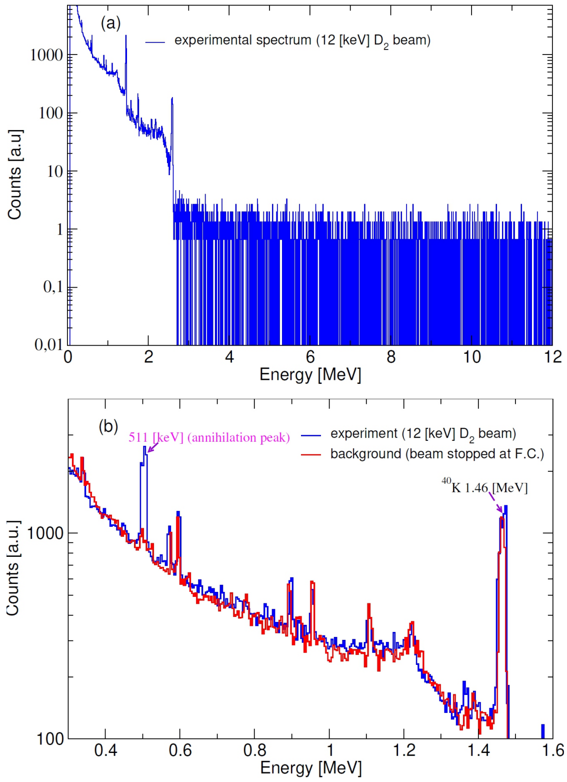

Fig. 3. (a) Blue curve represents the effect obtained during irradiation (12 keV deuteron beam) of the deuterated Zr target. (b) Low-energy gamma spectra measured with HPGe detector. The spectrum obtained for the deuterated Zr target irradiated with a 12 keV deuteron beam is compared to background measurements with the ion beam on the Faraday cup.

3. Discussion

The deuterium–deuterium (DD) fusion reaction has three known exit channels: two nearly equally probable channels — the neutron channel (^{3}H, n) and the proton channel (^{3}He, p) — and the significantly weaker gamma channel (^{4}He, γ). In the past two years, we have begun investigating the possible presence of a new "electron" channel, following the first observation of high-energy electrons in low-energy DD reactions [5]. We first attempted to experimentally estimate the total e^+e^- yield in 4π steradians during the reaction by measuring protons and ^{3}He using a 100 μm-thin Si detector placed very close to the target at a 12 keV deuteron beam. Later, solid angle and efficiency corrections were incorporated with the help of Geant4 Monte Carlo simulations. Further, we determined the branching ratios for the ^{3}He-proton, electron–proton, and positron–proton channels for deuteron energies of 12 keV. This is achieved using thick and thin Si detectors with various Al absorber foils, for example as shown in Fig. 2a. The methodology for calculating these branching ratios is thoroughly discussed in our recent studies [5, 11].

Table II presents the experimental data on the electron–proton branching ratio and compared with theoretical calculations from the references [5, 6], taking into account (or neglecting) the interference effect between the threshold resonance and the known broad resonances in the compound nucleus ^{4}He.

The experimentally observed increase of the electron–proton branching ratio for lowering deuteron energies could be explained by the IPC partial resonance width of about 140 meV, which is more than three times larger than the width of the proton partialresonance. This result agrees with the theoretical prediction of the IPC transition strength based on the energy weighted E_0 sum rule [6]. The presented approach of measuring the electron–proton branching ratio is independent of the electron screening effect, which affects the penetration factor through the Coulomb barrier, being equal for both studied channels and is eliminated from the branching ratio expression. More exact data are expected for measurements of branching ratio for deuteron energies below 5 keV, which will be very difficult because of the decreasing cross-section values. Theoretically, extrapolating our observations to energies of a few hundred eV, using the effective screening energy approach and parameters determined in existing accelerator experiments, indicates a slight increase in cross-sections. The absolute values of the cross-sections at these limits strongly depend on the screening energy, increasing by many orders of magnitude for the screened and resonance cross-sections, as reported by [5].

4. Conclusions

The present work may have significant consequences in both fundamental and applied sciences. For example, extending studies on the discovery of a new, strong electron reaction channel in deuteron–deuteron fusion at very low energies could lead to the feasibility of exploring metal hydride-based construction for future clean and efficient energy sources. Additionally, it could contribute to the modeling of nucleosynthesis in stars, particularly in the context of astrophysical strongly coupled plasmas, as well as to the fundamental study of few-nucleon systems using realistic nucleon–nucleon interactions, which have not included electron emission channels so far.

Acknowledgments

This project has received funding from the European Union's Horizon 2020 research and innovation programme under grant agreement No. 951974.

References

[1] W.A. Fowler, *Rev. Mod. Phys.* **56**, 149 (1984).

[2] C. Rolfs, W.S. Rodney, *Cauldrons in the Cosmos*, University of Chicago Press, Chicago 1988.

[3] S. Ichimaru, H. Kitamura, *Phys. Plasmas* **6**, 2649 (1999).

[4] K. Czerski, D. Weissbach, A.I. Kilic, G. Ruprecht, A. Huke, M. Kaczmarski, N. Targosz-Ślęczka, K. Maass, *Europhys. Lett.* **113**, 22001 (2016).

[5] K. Czerski, R. Dubey, M. Kaczmarski, A. Kowalska, N. Targosz-Ślęczka, G. Das Haridas, M. Valat, *Phys. Rev. C* **109**, L021601 (2024).

[6] K. Czerski, *Phys. Rev. C* **106**, L011601 (2022).

[7] R. Dubey, K. Czerski, H. Gokul Das, A. Kowalska, N. Targosz-Ślęczka, M. Kaczmarski, M. Valat, arXiv:2408.07567, under review for publication in *Nat. Commun.*, 2024.

[8] S. Kegel, P. Achenbach, S. Bacca et al., *Phys. Rev. Lett.* **130**, 152502 (2023).

[9] N. Michel, W. Nazarewicz, M. Płoszajczak, *Phys. Rev. Lett.* **131**, 242502 (2023).

[10] S. Agostinelli, J. Allison, K. Amako et al., *Nucl. Instrum. Method A* **506**, 186 (2003).

[11] H. Gokul Das, R. Dubey, K. Czerski, M. Kaczmarski, A. Kowalska, N. Targosz-Ślęczka, M. Valat, *Measurement* **228**, 114392 (2024).

[12] M. Kaczmarski, A.I. Kilic, K. Czerski et al., *Acta Phys. Pol. B* **45**, 509 (2014).

[13] A. Kowalska, K. Czerski, P. Horodek et al., *Materials* **16**, 6255 (2023).

[14] R. Dubey, K. Czerski, H. Gokul Das, M. Kaczmarski, A. Kowalska, N. Targosz-Ślęczka, M. Valat, *Acta Phys. Pol. B* **17**, 3-A35 (2024).

[15] CleanHME Report, Private communication.

[16] C. Iliadis, *Nuclear Physics of Stars*, Wiley, Berlin 2015, Ch. 4, p. 323.